

Magnetic properties of Fe-Mn-Al alloys in the disordered phase

G. A. Perez Alcazar,* J. A. Plascak, and E. Galvão da Silva
 Departamento de Física, Universidade Federal de Minas Gerais CP 702,
 30161 Belo Horizonte, Minas Gerais, Brazil

(Received 15 May 1987)

The magnetic properties of Fe-Mn-Al alloys in the disordered phase are investigated through the Mössbauer technique. The magnetic phase diagram in the bcc structural phase is obtained as a function of the Al concentration (q) and Mn concentration (x). The site-diluted Ising model proposed in a previous study of the Fe-Al system is extended to the present ternary alloy. Rather good fits of the experimental phase diagram, as well as the mean hyperfine field as a function of concentrations q and x , are obtained by using the same fitted values for the parameters of the exchange interaction $J(q)$ of the Fe-Al binary system.

In 1977 Chakrabarti,¹ by using x-ray diffraction, studied the structural phase diagram of the ternary Fe-Mn-Al system for alloys quenched from 1000°C. The phase diagram, shown in Fig. 1, exhibits two principal phases: the γ phase with crystalline fcc structure, which is stable for small Al concentrations and less than 60 at.% of Mn, and the α phase with bcc structure, which is stable for large Al concentrations and more than 45 at.% of Fe. This alloy system is intensively investigated because of the possibility of its application as a stainless steel. Although its structural and mechanical properties are well known, its magnetic properties have not been investigated to the same degree. Most of the studies found in the literature deal with the magnetic properties of the binary Fe-Mn (Refs. 2-7) and Fe-Al (Refs. 8-13) alloys. In particular, for the Fe-Al system, there has been recently reported¹⁴⁻¹⁶ a study of the magnetic properties of alloys prepared by the same heat treatment utilized by Chakrabarti. It has been shown that with this heat treatment it is

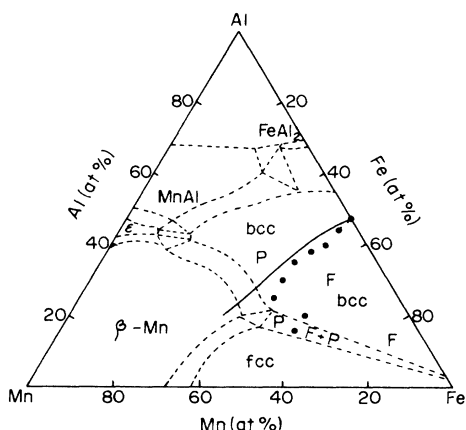


FIG. 1. Phase diagram of the ternary Fe-Mn-Al system. Dashed lines represent structural transitions (after Chakrabarti, Ref. 1). The dots represent the experimental results of the ferromagnetic (F) to paramagnetic (P) transition in the bcc structure. The solid line represents the theoretical result for the ferromagnetic transition line according to the model discussed in the text.

possible to extend the solid solubility of Al in the bcc Fe phase up to 47.5 at.% at room temperature (RT) and at the same time to maintain the disordered ferromagnetic phase. Moreover, it has been observed that the mean magnetic hyperfine field (HF) decreases gradually with Al concentration without exhibiting the anomalous behavior of the ordered Fe-Al system.⁸ Quite good fits of the experimental data of the mean HF and transition temperatures have also been obtained by using a simple site-diluted Ising model.¹⁴

In the present work we report a study of the Fe-Mn-Al disordered system in the bcc phase through the Mössbauer technique and x-ray diffraction. We also extend the site-diluted Ising model previously proposed for the binary Fe-Al alloys in order to describe the experimental results for the HF and critical concentrations of the ternary Fe-Mn-Al alloy. As far as we know, this is the first time that a magnetic phase diagram for this system is presented.

The alloys were prepared by employing Fe, Mn, and Al with better than 99.9% purity in a series of samples with concentrations of Al (q) or Mn (x) held constant. They were melted in an arc furnace in an argon atmosphere, then encapsulated in quartz tubes (previously evacuated) to be homogenized by annealing at 1000°C for a week followed by quenching in ice water. For the Mössbauer and x-ray measurements we used powder samples. The Mössbauer spectra were fitted with the hyperfine field distribution.

Several alloys were prepared and studied for different q or x until the critical concentration was obtained. Typical Mössbauer spectra at room temperature of two series of alloys samples and their respective HF distributions are shown in Figs. 2 and 3. In Fig. 2 we have samples with a constant Mn concentration $x=0.05$ and different Al concentrations q . In Fig. 3 we have samples with $q=0.25$ and different Mn concentrations x . In each spectrum is also shown the fitted average hyperfine field, \bar{H} , which was calculated by the expression

$$\bar{H} = \sum_i P_i(H_i)H_i, \quad H_{\min} < H_i < H_{\max}, \quad (1)$$

where H_{\min} and H_{\max} are the minimum and maximum HF and $P_i(H_i)$ is the calculated probability associated

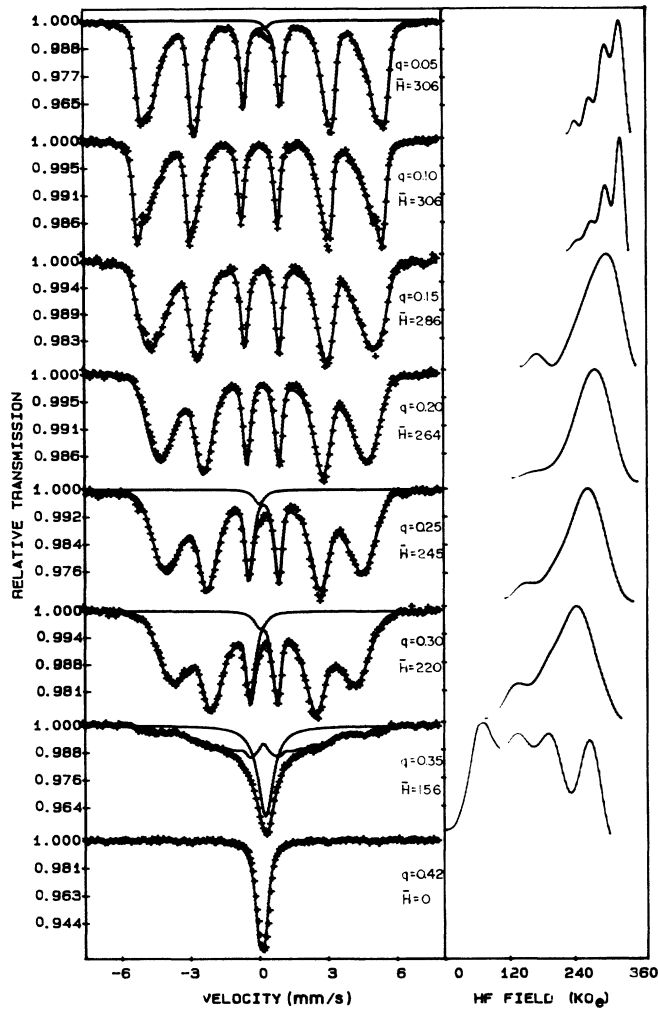


FIG. 2. Room-temperature Mössbauer spectra for alloys in the bcc phase with constant Mn concentration $x=0.05$ and the respective hyperfine field (HF) distribution for various Al concentrations q . \bar{H} is the average magnetic hyperfine field (in kOe).

with the magnetic field H_i . The general behavior of the HF distributions with increasing q or x is similar to those reported for disordered ferromagnetic Fe-Al alloys.¹⁵ Initially, we have several well resolved peaks, then the HF distribution collapses to a Gaussian form, and finally, near the critical concentration, the peaks appear again but shifted to small field values. In Figs. 4 and 5 we show the dependence of the fitted mean reduced HF at room temperature, $\bar{H}(\text{RT})/\bar{H}(0)$, where $\bar{H}(0)=340$ kOe is the Fe hyperfine field at 0 K. We can note that, in general, \bar{H} decreases gradually with q or x , except for $q=0.2$ and 0.25 for which \bar{H} decreases suddenly for large x . In the same figures are plotted the theoretical mean reduced HF which will be discussed later.

The x-ray diffraction results have shown that all the alloy samples have bcc structure as proposed by Chakrabarti. Moreover, as can be seen from Figs. 4 and 5, the lattice parameter increases linearly with increasing q while it is approximately constant with increasing x . This behavior is mainly due to the larger atomic size of Al and the

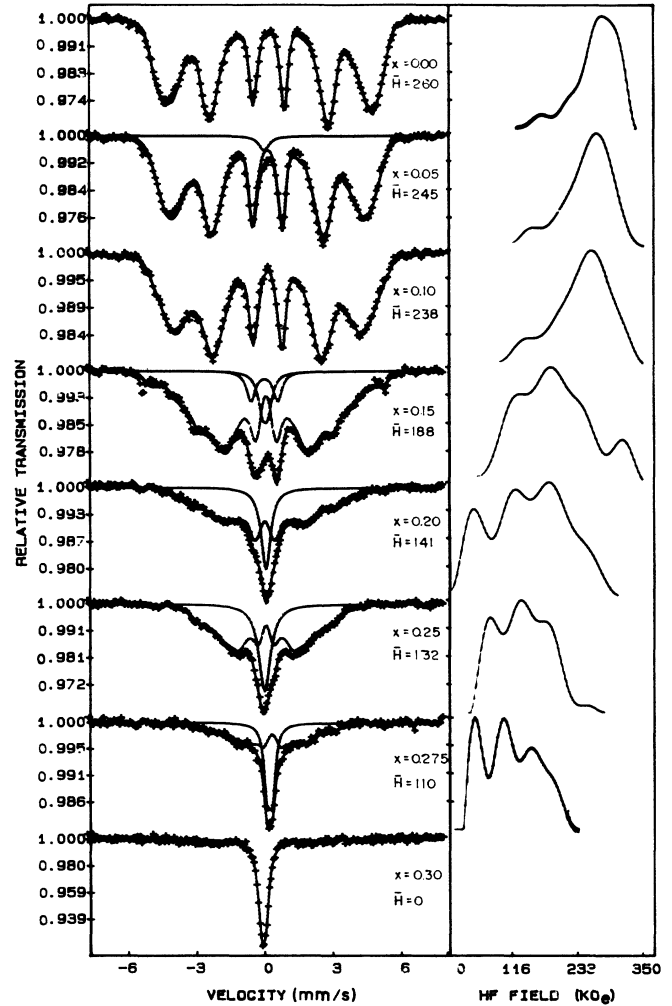


FIG. 3. The same as Fig. 2 for constant Al concentration $q=0.25$ and various Mn concentrations x .

similar atomic size of Mn in relation to Fe, respectively.

In order to verify the degree of disorder evidenced by the Mössbauer spectra and to obtain more information about this system, we have fitted the experimental results to a theoretical HF distribution. We have considered that the probability of finding n Al atoms and $0 < i < 8 - n$ Mn atoms as nearest neighbors (NN) of Fe, and m Al atoms and $0 < j < 6 - m$ Mn atoms as next-nearest neighbors (NNN) is given by the binomial distribution

$$P(n, m, i, j) = C_8^n C_6^m C_8^{i-n} C_6^{j-m} q^{n+m} x^{i+j} p^{14-n-m-i-j}, \quad (2)$$

where C_i^j are the binomial coefficients and $p=1-q-x$ is the Fe concentration. We associated with each configuration a HF given by the empirical expression

$$H = H_0(1 - \alpha n - \beta m - \gamma i - \delta j), \quad (3)$$

where $H_0=330$ kOe is the Fe magnetic hyperfine field at room temperature, α and β are the decreasing factors of H obtained by the substitution of one Fe for one Al atom in the first and second neighborhood, respectively, and γ and

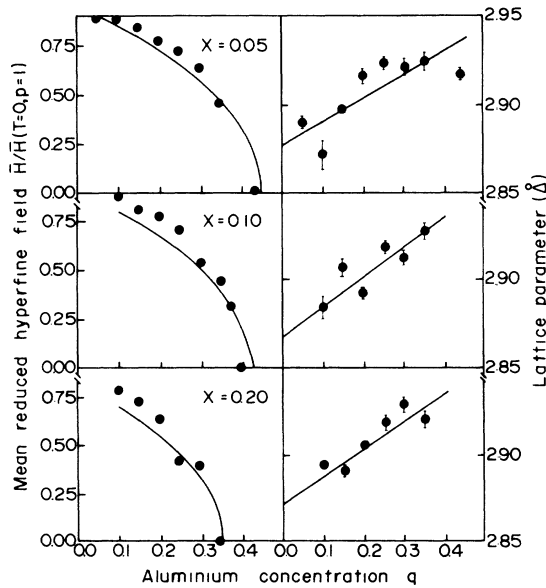


FIG. 4. Experimental (dots) and theoretical (solid line) mean reduced HF as a function of the Al concentration q , for different Mn concentrations x . The lattice parameter as a function of q is also shown in this figure.

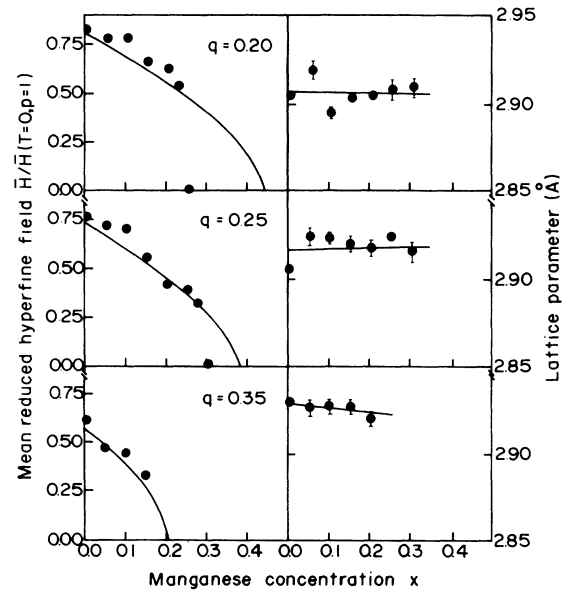


FIG. 5. Experimental (dots) and theoretical (solid line) mean reduced HF as a function of Mn concentration x , for different Al concentrations q . The lattice parameter as a function of x is also shown in this figure.

δ are the same factors for the Mn substitution. Equation (3) shows a linear decrease of H with n , m , i , or j and is valid only for small solute concentrations. In the present work we have used the same values $\alpha=0.0727$ and $\beta=0.015$ previously obtained for the Fe-Al alloys,¹⁵ which show a decrease $\Delta H_1=24$ kOe and $\Delta H_2=5$ kOe when one Fe atom is substituted for one Al atom in the first and second neighborhood, respectively. The values of γ and δ were adjusted in order to obtain the best fit of the theoretical HF distribution with the experimental ones. The mean values obtained are $\gamma=0.073$ and $\delta=0.008$, which correspond to $\Delta H_1=25.5$ kOe and $\Delta H_2=2.7$ kOe, respectively. The value of γ is in good agreement with that reported by Stearns,³ while that of δ is smaller. For larger Al or Mn concentrations we have not obtained a good fit; the experimental HF distributions are more shifted to small HF than the theoretical ones. In order to improve the fit it should be necessary to take into account the concentration dependence in Eq. (3). However, the good fit for small solute concentration is evidence that the alloy samples in that region form a random solid solution.

In order to obtain the magnetic properties of the Fe-Mn-Al disordered system, we have assumed the same quenched site-diluted Ising model with only NN interactions as has been proposed in the study of the Fe-Al alloys.¹⁴ The Hamiltonian can be defined as

$$H = - \sum_{(i,j)} J_{ij} \sigma_i \sigma_j, \quad (4)$$

where $J_{ij} > 0$ is the exchange parameter between NN spins and $\sigma_i = \pm 1$. The site dilution has the following probability distribution

$$P(\epsilon_i) = p\delta(\epsilon_i - 1) + (1-p)\delta(\epsilon_i), \quad (5)$$

where p is the ferromagnetic site concentration and $J_{ij} = J\epsilon_i\epsilon_j$ with $\epsilon_i = 1$ or 0 if the site i is occupied by a magnetic atom or not, respectively. The following experimental results reinforce the choice of the present model: (1) It has been found for Fe-Al disordered alloys¹⁵ that their disorder allows retention of the ferromagnetic exchange and an approximate constant magnetic moment up to the critical concentration. For these ternary Fe-Mn-Al disordered alloys we find the same behavior for the HF distributions and the mean HF as q or x increases. Therefore, we can use only one type of exchange parameter, $J_{ij} > 0$, a constant spin state, and a site-diluted model. (2) We consider only NN interactions because the studies of amorphous ferromagnetic alloys¹⁷ and disordered Fe-Al alloys¹⁵ show that the exchange parameter for the NNN J_2 is one order of magnitude smaller than that for the NN J_1 . For the present ternary alloys we find that the ratio between the reduction factors δ and γ is 0.13. Thus, as for the binary system, the choice of the Hamiltonian (4) is also strongly favored to describe the magnetic properties of the ternary Fe-Mn-Al alloy. Moreover, all the theoretical calculations done in Ref. 14 still hold in this case. We just have to take care of the fact that the exchange parameter $J = J(q) = J_1 - J_0q$ changes only with Al concentration q and remains constant with the Mn concentration x (see Figs. 4 and 5).

By using Eqs. (8), (9), (14), and (17) of Ref. 14 and the same adjusted values for the parameters of the Fe-Al system, namely, $J_1 = 12.846$ MeV and $J_0/J_1 = 0.95$, we have obtained the solid lines in Figs. 4 and 5 for the mean reduced HF as a function of q and x . One clearly notes a rather good fit to the experimental data for constant Mn concentrations $x \leq 0.2$ and Al concentrations $q > 0.3$. For low Al concentrations, which implies a higher Mn

concentration to destroy the magnetic order at RT, the experimental results go to zero more rapidly than the theoretical ones. This is more apparent in the phase diagram shown in Fig. 1. The theoretical curve is always above the experimental data mainly for $q \approx 0.3$ and $x \approx 0.2$ where an anomalous region is observed. This anomaly can be associated with the following: (i) As has been reported for the binary Fe-Mn alloy,^{5,6} for large Mn concentrations, Mn induces an antiferromagnetic interaction. In the present case, for $x \leq 0.2$ this interaction should be zero or nearly zero. However, as x increases, Mn can effectively exhibit an extra competitive antiferromagnetic interaction with Fe atoms. (ii) Ordered alloys can exist in this concentration region and the small HF observed experimentally in this case may be a consequence of the small effective number of magnetic NN. Then, the observed discrepancy between the theoretical and experimental results in the anomalous region shown in Fig. 1 is not surprising since the site-diluted model

given by Eq. (4) does not take into account either of the features described in (i) or (ii) above. However, it is interesting to notice that for small Mn concentration the present simple model can be easily extended to account for the main magnetic properties of the ternary Fe-Mn-Al system by using the same adjusted values of the parameters J_1 and J_0/J_1 previously obtained for the Fe-Al system. The anomalous region in the phase diagram, as well as the antiferromagnetic phase for low Al concentration in the fcc structure should be studied in more detail. Experimental and theoretical work in this direction is now in progress.

This work was partially supported by the Brazilian agencies Conselho Nacional de Desenvolvimento Científico e Tecnológico (CNPq), Financiadora de Estudos e Projetos (Finep), and Coordenação de Aperfeiçoamento de Pessoal de Nível Superior (Capes).

*Permanent address: Departamento de Física, Universidad del Valle, A.A. 25360, Cali, Colombia.

¹D. J. Chakrabarti, *Metall. Trans. B* **8**, 121 (1977).

²M. Hansen, in *Constitution of Binary Alloys* (McGraw-Hill, New York, 1958), p. 664.

³M. B. Stearns, *Phys. Rev.* **147**, 439 (1966).

⁴A. Umebayashi and Y. Ishikawa, *J. Phys. Soc. Jpn.* **21**, 1281 (1967).

⁵Y. Ishikawa and Y. Endoh, *J. Phys. Soc. Jpn.* **23**, 205 (1967).

⁶Y. Endoh and Y. Ishikawa, *J. Phys. Soc. Jpn.* **30**, 1614 (1971).

⁷S. G. Gang, H. Onodera, H. Yamamoto, and H. Watanabe, *J. Phys. Soc. Jpn.* **36**, 975 (1974).

⁸A. Arrot and H. Sato, *Phys. Rev.* **114**, 1420 (1959); **114**, 1427 (1959).

⁹J. Pickart and R. Nathans, *Phys. Rev.* **123**, 1163 (1961).

¹⁰G. P. Huffman and R. M. Fisher, *J. Appl. Phys.* **38**, 735 (1967).

¹¹G. P. Huffman, in *Amorphous Magnetism*, edited by H. D. Hooper and A. M. de Graaf (Plenum, New York, 1973), p. 283.

¹²M. Shiga and Y. Nakamura, *J. Phys. Soc. Jpn.* **40**, 5 (1976).

¹³R. D. Shull, H. Okamoto, and P. A. Beck, *Solid State Commun.* **18**, 211 (1976).

¹⁴G. A. Perez Alcazar, J. A. Plascak, and E. Galvão de Silva, *Phys. Rev. B* **34**, 1940 (1986).

¹⁵G. A. Perez Alcazar and E. Galvão da Silva, *J. Phys. F* **17**, 2323 (1987).

¹⁶H. Chacham, E. Galvão da Silva, D. Guenzburger, and D. E. Ellis, *Phys. Rev. B* **35**, 1602 (1987).

¹⁷S. N. Kaul, *Phys. Rev. B* **27**, 5761 (1983).